International Journal of Nanomedicine

Dovepress
open access to scientific and medical research

Open Access Full Text Article

ORIGINAL RESEARCH

A novel bacterial cellulose membrane immobilized with human umbilical cord mesenchymal stem cells-derived exosome prevents epidural fibrosis

This article was published in the following Dove Press journal:
International Journal of Nanomedicine

Bo Wang,[1,*] Peng Li,[1,*] Lei Shangguan,[2,*] Jun Ma,[3,*] Kezheng Mao,[4] Quan Zhang,[5] Yiguo Wang,[6] Zhongyang Liu,[1,2] Keya Mao[1]

[1]Department of Orthopedics, Chinese PLA General Hospital, Beijing, 100853, China; [2]Department of Orthopedics, Xijing Hospital, Fourth Military Medical University, Xi'an, Shaanxi, 710032, China; [3]Department of Orthopedics Trauma Surgery, Changzheng Hospital, Second Military Medical University, Shanghai, 200003, China; [4]Department of Orthopedics, Orthopedics Hospital of Zhengzhou City, Zhengzhou, Henan, 450052, China; [5]Department of Orthopedics, People's Hospital of Tianjin City, Tianjin, 300121, China; [6]Department of Orthopedics, Second Affiliated Hospital of Nanjing Medical University, Nanjing, Jiangsu, 210000, China

*These authors contributed equally to this work

Correspondence: Zhongyang Liu
Department of Orthopedics, Chinese PLA General Hospital, No. 28 Fuxing Road, Haidian District, Beijing, 100853, China
Email lzy_westlife@163.com

Keya Mao
Department of Orthopedics, Chinese PLA General Hospital, No. 28 Fuxing Road, Haidian District, Beijing 100853, China
Tel +86 10 6693 9439
Fax +86 10 8821 9862
Email maokeya@sina.com

Introduction: Failed back surgery syndrome is a situation where there is failure after lumbar surgery aimed at correcting lumbar disease that is characterized by continuous back and/or leg pain. Epidural fibrosis and adhesions are among the major causes of failed back surgery syndrome. In recent years, several biomaterials have been applied as barriers or deterrents to prevent the compression of neural structures by postsurgical fibrosis.

Methods: In this study, a new bacterial cellulose (BC) anti-adhesion membrane, composed of exosomes from human umbilical cord mesenchymal stem cells, was developed. Its structure and morphology, water content, thickness, and mechanical properties of elasticity were analyzed and characterized. The degradation of the BC+exosomes (BC+Exos) membrane in vitro was evaluated, and its in vitro cytotoxicity and in vivo biocompatibility were tested. The prevention effect of BC+Exos membrane on epidural fibrosis post-laminectomy in a rabbit model was investigated.

Results: The BC+Exos membrane showed a three-dimensional network structure constituted of high-purity cellulose and moderate mechanical properties. No degeneration was observed. The BC+Exos membrane showed no cytotoxicity and displayed biocompatibility in vivo. The BC+Exos film was able to inhibit epidural fibrosis and peridural adhesions.

Conclusion: Based on the current findings, the BC+Exos membrane is a promising material to prevent postoperative epidural fibrosis and adhesion.

Keywords: failed back surgery syndrome, epidural fibrosis, adhesion, human umbilical cord mesenchymal stem cell, exosome, bacterial cellulose

Introduction

Failed back surgery syndrome (FBSS) is a cluster of symptoms characterized by intractable or recurrent pain in the back or limbs after laminectomy.[1] Epidural fibrosis and adhesion are among the main causes of FBSS and may lead to the continuing compression of dura and nerve roots, introduce chronic nerve radicular pain, and lower extremity weakness in as much as 24% of affected patients.[2] Moreover, the existence of epidural adhesion makes reoperation cases more difficult, because of the higher risk of dural tears, nerve root injury, bleeding, and iatrogenic instability.[3] Driven by the above issues, the introduction of physical barriers to isolate the epidural, nerve root, and rear tissue is considered to be the most effective way to reduce epidural tissue adhesion and prevent epidural fibrosis.

To date, most biomaterials, such as Adcon-L gel, carboxymethylcellulose/polyethylene oxide, polyethylene glycol hydrogel, hyaluronic acid, and poly L-glutamic acid/chitosan composite, have been applied in preventing epidural fibrosis.[4–8] However, pain, tachycardia, skin erythema, high cost, and suboptimal prevention of epidural fibrosis have restricted their further application in practice.[9,10] Therefore, it is urgent

submit your manuscript | www.dovepress.com
Dovepress
http://dx.doi.org/10.2147/IJN.S167880

to explore a simple and convenient method to fabricate a tunable material in the prevention of epidural fibrosis. In recent years, human umbilical cord mesenchymal stem cells (HUCMSCs)-based therapy has been introduced for the prevention of several fibrosis pathologies[11,12] because of their easy isolation, large yields, and immunosuppressive activities.[13,14] However, several limitations have been found in the application of HUCMSCs such as a long cell incubation period, phenotype changes during cell proliferation, and a low survival number of locally transplanted cells.[15] Therefore, various technologies had been put into practice to eliminate these limitations. Recent studies have shown that the positive therapeutic outcomes of HUCMSCs were mainly dependent on paracrine mechanisms, such as conditioned medium and extracellular vesicles, rather than direct cell transplantation.[16,17]

Exosomes – a type of extracellular vesicles – have been proved to be important for cellular functions;[18–20] they are a specific kind of membrane vesicles measuring 40–150 nm in diameter.[21] Moreover, evidence shows that these exosomes are actually a crucial transmitter in cell-to-cell communication, and play vital roles in normal physiological processes and diseases, such as hepatic fibrosis, myocardial fibrosis, and renal fibrosis.[22–25] However, it is still unclear whether exosomes from HUCMSCs, combined with biomaterials, can modulate epidural fibrosis after lumbar surgery.

Here, we fabricated a membrane biomaterial which consisted of bacterial cellulose (BC) membrane and HUCMSCs-Exos. We first characterized the physical and chemical properties of the BC+Exos membrane. Then, the biocompatibility and biodegradation – both in vitro and in vivo – were analyzed. Most importantly, prevention of epidural fibrosis and adhesion by the BC+Exos membrane was observed in laminectomy rabbit models.

Materials and methods

Cell culture from human umbilical cords

Human umbilical cords were obtained from the Chinese PLA General Hospital, with approval by the ethics committee, and written informed consent was obtained from three pregnant women (age range 25–27 years) whose umbilical cords, after cesarean delivery, were used in this study. A primary culture of HUCMSCs was established by the standard procedure. Briefly, umbilical cords were first washed with 75% ethanol and then with DMEM (Thermo Fisher Scientific, Waltham, MA, USA) containing 1% L-glutamine, 10% fetal bovine serum (FBS; Thermo Fisher Scientific), and antibiotics (100 μg/mL streptomycin and penicillin solution). After removing excess blood, the umbilical cords were cut into small pieces (3–5 mm) and incubated with medium at 37°C with 5% CO_2. When the HUCMSCs reached 80%–90% confluence, they were trypsinized and prepared for subculture. Thereafter, HUCMSCs that were passaged no more than five times were used in the remainder of the experiment. The morphological appearance of the cells was observed by light microscopy (Olympus Corporation, Tokyo, Japan).

Cluster of differentiation (CD) marker identification

The immunophenotypic characterization of HUCMSCs was analyzed by flow cytometry assay. In brief, HUCMSCs were trypsined for 2–4 minutes. Then, the cells were washed with PBS without magnesium and calcium and later blocked with 10% normal goat serum to prevent nonspecific binding. Next, the cells were incubated with a series of human monoclonal primary antibodies with fluorescein isothiocyanate (FITC) dyes for CD markers, including CD14, CD19, CD29, CD34, CD44, CD45, CD73, CD90, HLA-A,B,C, and HLA-DR (1:100; BioLegend, San Diego, CA, USA) for 30 minutes. Next, the cells were washed with PBS without calcium and magnesium, resuspended in 10% normal goat serum, and filtered to remove cell clusters before they were analyzed with a CyAn ADP Analyzer (Beckman Coulter, Brea, CA, USA).

Cell multi-differentiation

For osteogenic differentiation, HUCMSCs were seeded (1×10^5 cells/well) into six-well culture plates and cultured for 1 day to allow attachment, and the substrate was then switched to osteogenic medium containing DMEM supplemented with 0.17 mM L-ascorbic acid, 5% FBS, 10 mM β-glycerophosphate, 100 nM dexamethasone (Sigma, St Louis, MO, USA), and 1% penicillin/streptomycin; then, the cells were incubated at 37°C with 5% CO_2 for 21–28 days with fresh osteogenic medium every 2 days. When the calcium nodules could be obviously observed by light microscopy, the cells were then subjected to Alizarin red S staining. In brief, the cell were washed with PBS two times and then fixed in 4% formaldehyde for 15 minutes. Later, the plates were washed with deionized water two times and stained in Alizarin red S solution for 30 minutes. The stained cells were then washed with deionized water two times and observed by using a light microscope (Olympus). For adipocyte differentiation, HUCMSCs were seeded into (1×10^5 cells/well) six-well culture plates and cultured for 1 day to allow attachment, and the substrate was then changed to a adipogenic differentiation cocktail comprising 1 μM

rosiglitazone, 1 μM dexamethasone, 0.5 mM 3-isobutyl-1-methyl-xanthine, 10 μg/mL insulin, 0.2 mM indomethacin, and 1% penicillin/streptomycin in DMEM-low glucose supplemented with glutamine and 10% FBS. After 3 days, the medium was changed by DMEM-Low glucose containing glutamine, 10% FBS, 1% penicillin streptomycin, 1 mM rosiglitazone, and 10 mg/mL insulin every other day. The cells were incubated at 37°C with 5% CO_2 for 21–28 days and when the lipid droplets were apparently visible under light microscopy, the cells were dyed by Oil Red O. Briefly, the cells were rinsed with deionized water and then fixed with 4% paraformaldehyde for 15 minutes and rinsed with PBS, and then with 65% isopropanol for 4 minutes. The cells were later dyed with new filtered Oil Red O for 4 minutes, washed with deionized water until the water ran as a liquid, and re-dyed with hematoxylin. The images were acquired on light microscopy (Olympus). For chondrogenic differentiation, HUCMSCs were seeded into a (2×10^6 cells/tube) 15-mL centrifuge tube in a ball-like structure and cultured at 37°C in 5% CO_2 for 24 hours, and the substrate was then switched to chondrogenic medium containing DMEM (4.5 g/L glucose) supplemented with 100 nM dexamethasone, 0.35 mM proline, 0.17 mM L-ascorbic acid, 1 mM sodium pyruvate, 1% insulin-transferrin-selenium, 10 ng/mL TGFβ-3 (Sigma), and 1% penicillin/streptomycin, and the cells incubated at 37°C with 5% CO_2 for 21–28 days with fresh changes of medium every 2 days. When the global cells were grown into balls with 1.5–2.0 mm diameter, the cells were sliced into pieces and dyed with Alcian Blue staining. Briefly, the cells were rinsed by using deionized water two times and fixed into 4% paraformaldehyde for 15 minutes. After rinsing with deionized water two times, the cells were cut into 10-μm frozen sections on glass slides. The slides were then rinsed with deionized water and stained with 0.5% Alcian Blue dye for 30 minutes. After washing with deionized water, the sections were photographed under light microscopy (Olympus).

Exosome purification and characterization

After 72 hours of HUCMSCs culture without FBS, debris and dead cells in the medium were removed by centrifugation at 1,200 × *g* for 25 minutes at 4°C and then filtered through a 0.2-mm filter. The medium was then subjected to ultra-centrifugation at 120,000 × *g* for 2.5 hours at 4°C. After washing with PBS (120,000 × *g* for 20 minutes), the exosome-containing pellet was resuspended in PBS. The characterization of exosomes was identified by evaluating the expression of specific markers HSP70, CD63, and CD9 by Western blotting analysis. The particle size distribution of exosomes was analyzed by Zetasizer Nano ZS (Malvern Instruments, Malvern, UK). For transmission electron microscopy, exosomes were loaded on Formvar and carbon-coated copper grids. Then, the grids were placed on 2% phosphotungstic acid for 1 minute and rinsed with PBS. The morphology of exosomes were acquired by using a transmission electron microscope (TEM; Tecnai Spirit; FEI, USA).

Preparation of the BC+Exos membrane

A static culture method was used to prepare BC. In total, 5 g yeast extract, 50 g sucrose, 3 g KH_2PO_4, 5 g $(NH_4)_2SO_4$, 0.8 g citric acid, 0.05 g $MgSO_4\cdot7H_2O$, and 1 g ethanol were dissolved in 1 L deionized water to prepare a fermentation medium, which was sterilized for 20 minutes at 121°C. Seed-culture solution was inoculated by recovered freeze-dried acetobacterxylinum (QAX993; Guang Yu Biomedical Corporation, China) at a volume equivalent to 10%. Then, 50 mL seed-culture solution was inoculated into a 250-mL Erlenmeyer flask that contained 50 mL fermentation substrate; the HUCMSCs-derived exosomes (HUCMSC-Exos) were added into the mixture and cultured for 7 days at 30°C in an electric thermostat incubator. Then, the membrane was extracted and immersed in 1% NaOH solution for 30 minutes to remove residual medium and bacteria. The film was rinsed with deionized water to neutral.

Characterization of the BC+Exos membrane

The chemical groups of the BC+Exos membranes were analyzed with Fourier transform infrared spectrometry (FTIR). The microscopic morphology of BC membranes was observed using an environmental scanning electron microscope (ESEM). Then, the water content of the BC membrane and BC+Exos membrane was analyzed. The membranes (15×30 mm) were removed from deionized water, the excess solution was wiped off by filter paper, and the membranes were then weighed (m_0). Thereafter, the same sample was dried to a constant weight (m_1). The water content (Q) was calculated with the following equation: $Q=(m_0-m_1)/m_0\times100\%$. Thirty samples were tested, and the mean value of Q was calculated. Next, we tested the tensile strength, elongation at break, and elastic modulus of the BC+Exos membrane. The membranes were cut into strips and the width (b, mm) and thickness (d, mm) of the samples were measured by electronic Vernier caliper. Then, the samples were then subjected to tensile tests using non-metallic material tensile-testing machine, and the initial length (L_0) and breaking length (L)

were recorded. Tensile strength (σ, MPa) was calculated by the following equation: $\sigma=F/(b\cdot d)$. F (N) was the maximum load when the specimen broke. Elongation at break (ε) was calculated using the following equation: $\varepsilon=(L-L_0)/L_0\times100\%$. Elastic modulus (E) was calculated according to Hooke's law: $\sigma=E\cdot\varepsilon$. The measurement was repeated for ten times, and mean values were calculated.

In vitro degradation rate of the BC+Exos membrane

The BC+Exos membranes with a size of 15×30 mm were dried to constant weight (W_0). Then, the membranes were immersed in tubes with simulated body fluids. The tubes were bathed in a 37°C water for different periods of time. The samples were taken out and rinsed several times with deionized water and dried to constant weight (W_1) in each month of the testing period. The differences in weight were statistically analyzed to assess the degradation of BC+Exos membranes. The degradation of BC membranes were conducted as described earlier.

Cytotoxicity test of the BC+Exos membrane in vitro

L929 fibroblast cells (American Type Culture Collection) – the main cells for testing the cytotoxicity of the biomaterials – were cultured in the culture plate, together with the BC membrane and BC+Exos membrane at 37°C in 5% CO_2. Eight plates cells were cultured in each group, and four of these were supplied for Cell Counting Kit 8 (CCK-8) assay and the other four were prepared for Live/Dead assays. In brief, the cell activity was examined and quantified with the CCK-8 (Dojino, Japan). At 24, 72, and 120 hours after culture, one of the four plates of L929 fibroblast cells in different concentration liquid extracts were rinsed with PBS three times. Thereafter, fibroblasts were trypsinized with a 0.05% trypsin solution, washed, and resuspended in DMEM. Then, the cell suspension was incubated (100 μL/well) in a 96-well plate. In total, 10 μL of the CCK-8 solution was added into each well and cultured for 4 hours. The absorbance value was detected at 492 nm. The Live/Dead (Bio Vision, USA) assays were conducted to assess the survival and proliferation of L929 fibroblasts seeded on the membranes. At 24, 72, and 120 hours after cell adhesion, 200 μL of fresh serum-free DMEM with 5 mM of Live-Dye and 5 mM of propidium iodide was added into the cell plate. A green fluorescent dye of Live-Dye™ (excitation/emission 488/518 nm) was used to dye the live cells, and a red fluorescent dye of propidium iodide (excitation/emission 488/615 nm) was used to dye the dead cells. After incubation for 2 hours, the cells were rinsed with PBS three times, with an interval of 10 minutes to remove unbound reaction substrates. The bicolor labeling was observed by using a fluorescence microscope (FV-1000, Olympus). The images were analyzed with an FV10-ASW 3.1 viewer (Olympus).

Animal surgical procedure

The animal experiments were approved by the animal ethics committee of the People's Liberation Army (PLA) General Hospital (approval no 2013-X7-29), and all animal experiments were undertaken in conformity with the Guide for the Care and Use of Laboratory Animals (National Institutes of Health publication no 85-23, revised 1985).[26] A total of 270 New Zealand White rabbits (Animal Center, PLA General Hospital, Beijing), weighing 2.5–3.0 kg, were randomly divided into five groups as shown in Table 1. Ketamine hydrochloride (2 mL, 100 mg) and serotrazine hydrochloride

Table 1 Number of rabbits per group

Experimental time point after surgery	Control group	ePTFE membrane group	PU membrane group	BC membrane group	BC+Exos membrane group
1 day					
Blood tests	10	–	–	10	10
3 days					
Blood tests	10	–	–	10	10
7 days					
Blood tests and histologic analysis Biocompatibility	10	–	–	10	10
30 days					
Blood tests	10	–		10	10
90 days					
Blood tests and MRI examination	10	10	10	10	10
1 year after					
General view and histologic analysis	20	20	20	20	20
Total number	70	30	30	70	70

Abbreviations: –, not applicable; BC, bacterial cellulose; BC+Exos, bacterial cellulose combined with exosomes; ePTFE, expanded polytetrafluoroethylene; PU, polyurethane.

(2 mL, 40 mg) were mixed in a 1:1 ratio as the anesthetic in the experiments. The operations were carried out under general anesthesia by intramuscular injection of the anesthetic mentioned above (0.4 mL/kg). The animals were fixed in the prone position and the surgical area was sterilized with povidone–iodine solution. An incision was made in the midline of the posterior skin. In the in vivo biocompatibility text group, two BC membranes (30×15 mm) were buried in the subcutaneous tissue and muscle. Then, the skin was closed with 4–0 nylon sutures. In the anti-adhesion test groups, the paraspinal muscles were stripped by electric scalpel and the spinous process, lamina, and upper and lower articular processes of L6 vertebrae were revealed. A laminectomy of L6 was conducted, and the ligamentum flavum and epidural fat were removed. The defect area of rabbits in the control group were not covered (control group), whereas the exposed dura site of animals in the intervention groups were covered with expanded polytetrafluoroethylene (ePTFE) film (ePTFE group; Gore Preclude; W.L. Gore & Associates, Inc., Newark, DE, USA), polyurethane (PU) patch (PU group; Neuro-Patch B. Braun), BC membrane (BC membrane group), or BC+Exos membrane (BC+Exos membrane group). The deep fascia and skin were sutured with 4–0 nylon sutures. Postoperatively, the rabbits were housed individually, received free access to water and food, and were allowed normal activity.

Blood tests in vivo

Blood tests of alanine transaminase (ALT), aspartate transaminase (AST), blood urea nitrogen (BUN), and serum creatinine (Scr) were carried out on animals of the anti-adhesion test groups 1 day before surgery (Day 0) and at days 1, 3, 7, 30, and 90 after surgery to assess the toxicity of the implants to liver and kidney. All the animals were fasted for 6 hours before blood collection from the marginal vein of the ear.

General observation and histologic examination

Ten animals of the in vivo biocompatibility text group were sacrificed postoperatively on Day 7. The tissues around the membranes were prepared for histological observation. The thin sections were evaluated after hematoxylin–eosin (HE) staining to examine the inflammatory reaction around the BC membranes. Moreover, the effect of the BC+Exos membrane on visceral organs (heart, liver, and kidney) was evaluated at 1 year post operation. The experimental rabbits in the anti-adhesion text groups were sacrificed 1 year after surgery to assess the adhesion extent between the dura mater and surrounding soft tissues. Peridural adhesion grades were evaluated blindly according to the difficulty of separation of the scar tissue and dura mater,[27] which are summarized in Table 2. Then, the surgical spine segments were resected en bloc, fixed in a 4% formalin solution and decalcified. Following this step, the vertebral columns were sectioned horizontally and stained with HE, Masson trichrome, and Sirius red, and the microscopic images were photographed. Peridural fibrosis and adhesions were assessed on the basis of the adhesions grading scale previously described by Lo et al (Table 2).[28] All of the above experiments were conducted by an experienced observer who was blinded to the experiment, with blinding used to prevent subjective bias.

Magnetic resonance imaging (MRI) examination

The animals in the anti-adhesion text groups underwent MRI examination at 3 months post-surgery in a 1.5 T MRI scanner. After general anesthesia, spin echo T1-weighted (TR_540 ms, TE_26 ms) and gradient-recalled echo T2-weighted (TR_1800 ms, TE_80 ms) images at the laminectomy level of the rabbits were acquired, both in sagittal and transverse planes.

Gene expression experiment

At 4, 8, and 12 months after surgery, the tissues around the surgical area were first harvested and the total RNA was extracted from the tissues by adding TRIzol reagent (Sigma-Aldrich). The expression levels of collagen type I (COL I), collagen type III (COL III), and alpha smooth muscle actin (α-SMA) messenger RNA (mRNA) were determined by quantitative real-time PCR (qRT-PCR) analysis. The sequencers of primers for COL I, COL III, α-SMA, and ACTB (internal control) are shown in Table 3. The experimental conditions for qRT-PCR were as follows: denaturation at 95°C, 45 seconds; primer annealing at 55°C, 30 seconds; and elongation at 60°C, 60 seconds. Quantification of PCR products was analyzed using the $2^{-\Delta\Delta Ct}$ approach. The relative gene expression levels of mRNA were normalized to the corresponding gene ACTB. Three replicates were done using triplicate wells. The healthy (unwounded)

Table 2 The number of rabbits in different adhesion grades

Groups	Adhesion grades				
	0	I	2	3	4
Control group	0	0	0	3	17
ePTFE membrane group	8	5	5	2	0
PU membrane group	7	5	6	I	0
BC membrane group	9	9	2	0	0
BC+Exos membrane group	18	2	0	0	0

Abbreviations: BC, bacterial cellulose; BC+Exos, bacterial cellulose combined with exosomes; ePTFE, expanded polytetrafluoroethylene; PU, polyurethane.

Table 3 Primer sequences used for the real-time PCR

Gene	Direction	Sequence	GenBank accession number
COL I	Upper	5′ GCCACCTGCCAGTCTTTACA 3′	NM_001195668.1
	Lower	5′ CCATCATCACCATCTCTGCCT 3′	
COL III	Upper	5′ AAAGAAAGCCCTGAAGCTGATG 3′	XM_002712333
	Lower	5′ CCACCAATATCATAGGGTGCAA 3′	
α-SMA	Upper	5′ ACCGTATGCAGAAGGAAATCA 3′	NM_001101682
	Lower	5′ GCTAGAAACAGAGCAGGGAAGT 3′	
Actb	Upper	5′ CTGCGTCTGGACCTGGATGG 3′	NM_002712153
	Lower	5′ CGATGGTGATGACCTGGCTGT 3′	

Abbreviations: COL I, collagen type I; COL III, collagen type III; α-SMA, alpha smooth muscle actin; Actb, β-actin.

rabbits and the wounded rabbits without membrane covered served as controls.

Statistical analysis

Data were expressed as mean ± standard error of mean and analyzed with the SPSS 20.0 statistical package. The differences of quantitative variables were determined by variance analysis, and the differences of qualitative variables between groups were evaluated with chi-squared test or Wilcoxon rank sum test. Values of $P<0.05$ were considered statistically significant.

Results

Identification of HUCMSCs and exosome

The expression of cell surface markers were identified by flow cytometric analysis. Figure 1A showed that the cells expressed typical CD marker profiles of HUCMSCs: positive for CD29, CD44, CD73, CD90, and HLA-A,B,C; but negative for CD14, CD19, CD34, CD45, and HLA-DR. The morphological appearance of the cells was observed under light microscopy (Figure 1B). Figure 1C–E shows that the cells were capable of osteogenic, adipogenic, and chondrogenic differentiation, respectively. These results suggested that the cells were HUCMSCs. Next, the characterization of exosomes from HUCMSCs was undertaken. The TEM image showed that the particle was a typical round-shaped membrane (Figure 1F), the sizes ranged from 40 to 150 nm, and the mean diameter was 61.58 nm (Figure 1G). Moreover, the representative markers of the exosome are observed in Figure 1H. Taken together, these results suggested that the HUCMSCs and exosome were suitable for the remaining experiments.

Characterization and morphology of the BC+Exos membrane

The general observation of the fabricated BC+Exos membrane was that it was neat, soft, and off a light white color (Figure 2B), in consistency with the BC membrane (Figure 2A). The IR spectra of the BC+Exos membrane is shown in Figure 2C. The IR spectrum of the BC+Exos membrane displayed a wide absorption band in the range of 3,500–3,000 cm^{-1}, which was due to the ν(O–H). A smaller absorption band at 2,990 cm^{-1} was attributable to ν(C–H). The main representative IR absorption band was observed at 1,000 cm^{-1}, which was consistent with the standard IR spectra of the cellulose, indicating that the main component of the film was cellulose. The BC membrane showed a similar IR spectrum, compared with the BC+Exos membrane. The morphology of the BC+Exos membrane was observed by SEM. Figure 2E showed that the BC+Exos membrane was composed of three-dimensional (3D) networks of fiber structure with high porosity, large internal 3D space, and even fiber diameter,[29] and the average diameter of the fibers was 25.25±1.05 μm (Figure 2F), suggesting that the BC+Exos membrane was capable of nutrient exchange and oxygen availability within the surrounding environment. Figure 2D showed that the BC membrane also expressed 3D networks of fibers and the mean diameter of fibers was 25.20±1.05 μm (Figure 2F), compared with the BC+Exos membrane.

Properties of the BC+Exos membrane

Next, we conducted the water content test to investigate the water content of the BC+Exos membrane. The results showed that the BC+Exos membrane and BC membrane had a high water content of 94.13%±1.89% and 94.29%±1.23% (Figure 3A), respectively, and the two groups had no significant difference. Moreover, the thickness of the BC+Exos membrane and the BC membrane was 0.80±0.07 and 0.81±0.06 mm, respectively. The tensile strength (σ) of the BC+Exos membrane and BC membrane was 3.15±0.42 MPa (Figure 3C) and 3.15±0.38 MPa (Figure 3B), respectively. The elongation of break (ε) in the BC+Exos membrane group and BC membrane group was 28.60%±3.59% and 28.81%±3.32% (Figure 3D), respectively. As described in

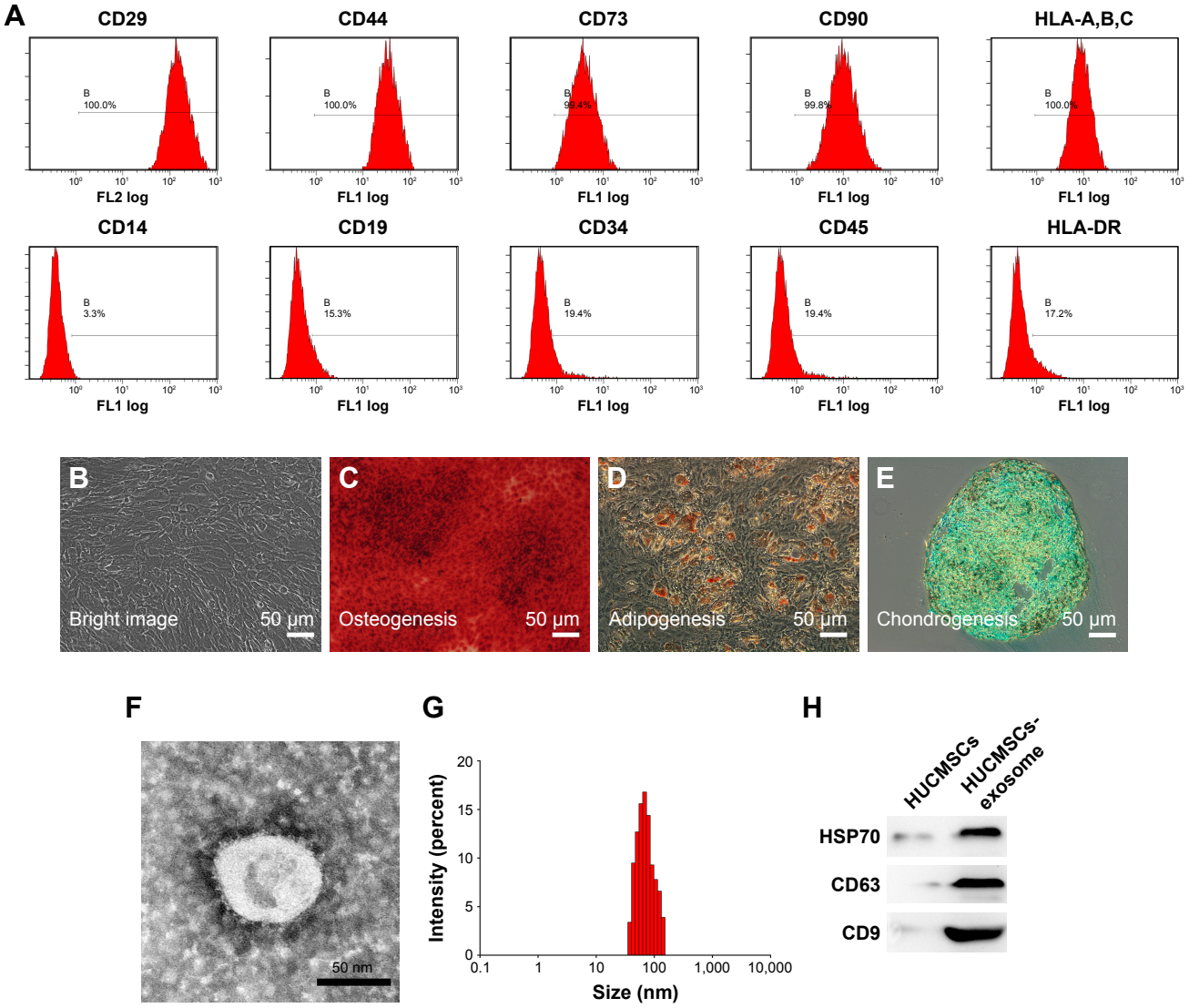

Figure 1 Identification of human umbilical cord mesenchymal stem cells (HUCMSCs) and HUCMSCs-derived exosomes.
Notes: (**A**) Flow cytometric analysis of the expression of cell surface markers related to HUCMSCs. (**B**) Bright image of HUCMSCs under a light microscope. (**C**) Representative image of osteocyte differentiation of HUCMSCs by using cytochemical staining with Alizarin Red. (**D**) Representative image of adiocyte differentiation of HUCMSCs by using cytochemical staining with Oil Red O. (**E**) Representative image of chondrocyte differentiation of HUCMSCs by using cytochemical staining with Alcian Blue. (**F**) Transmission electron microscopic image of HUCMSCs-exosome. (**G**) The size distribution of the HUCMSCs-exosome was analyzed by using a Zetasizer Nano ZS. (**H**) The positive markers for exosomes, HSP70, CD63, and CD9 were detected by using Western blotting.

a previous study, the tensile strength of the ePTFE conduit material (70×22 mm dimensions) was 7.70±0.43 MPa, which was much higher than that of healthy normal aortic walls and demonstrated excellent early clinical outcomes; moreover, the elongation of break of the material was 32.86%±6.71%,[30] which was close to that in the BC+Exos membrane in our study. Moreover, different lengths of ePTFE materials showed different mechanical properties and could alter the performance of the material.[31] Based on the mechanical experiments in our study, both the membranes (15×30 mm) had moderate cellulose crystallinity and mechanical strength. The elastic modulus of the BC+Exos membrane and BC membrane was 11.02±0.76 and 10.98±1.26 MPa (Figure 3E), which was close to the elastic modulus of articular cartilage.[32] All the findings indicated that the BC+Exos membranes we fabricated had moderate elasticity and adhesiveness and could tightly adhere to an irregular surface. The in vitro degradation of the membrane was evaluated by the weight changes before and after immersion in simulated body fluids. The weight loss was 0.005±0.002, 0.013±0.005, 0.024±0.009, 0.037±0.014, 0.048±0.018, and 0.066±0.025 g at 1, 2, 3, 4, 5, and 6 months in the BC+Exos membrane group, respectively. Moreover, the weight loss was 0.004±0.001, 0.011±0.002, 0.022±0.004, 0.033±0.007, 0.044±0.009, and 0.061±0.013 g at 1, 2, 3, 4, 5,

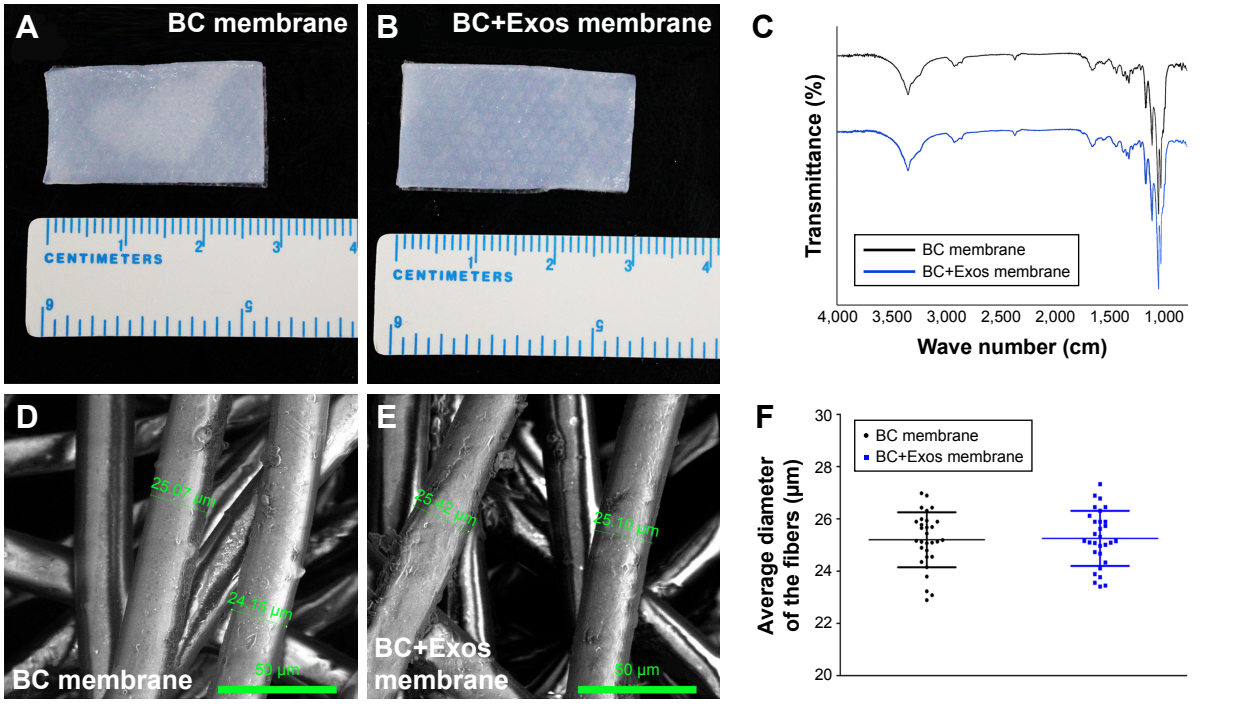

Figure 2 Characterization of the BC membrane and the BC+Exos membrane.
Notes: (**A** and **B**) The appearance of the BC membrane and the BC+Exos membrane, respectively. (**C**) The FTIR spectra of the BC membrane and BC+Exos membrane. (**D** and **E**) Representative images of the BC membrane and the BC+Exos membrane, respectively. (**F**) The average diameter of the fibers.
Abbreviations: BC, bacterial cellulose; BC+Exos, bacterial cellulose combined with exosomes; FTIR, Fourier transform infrared spectrometer.

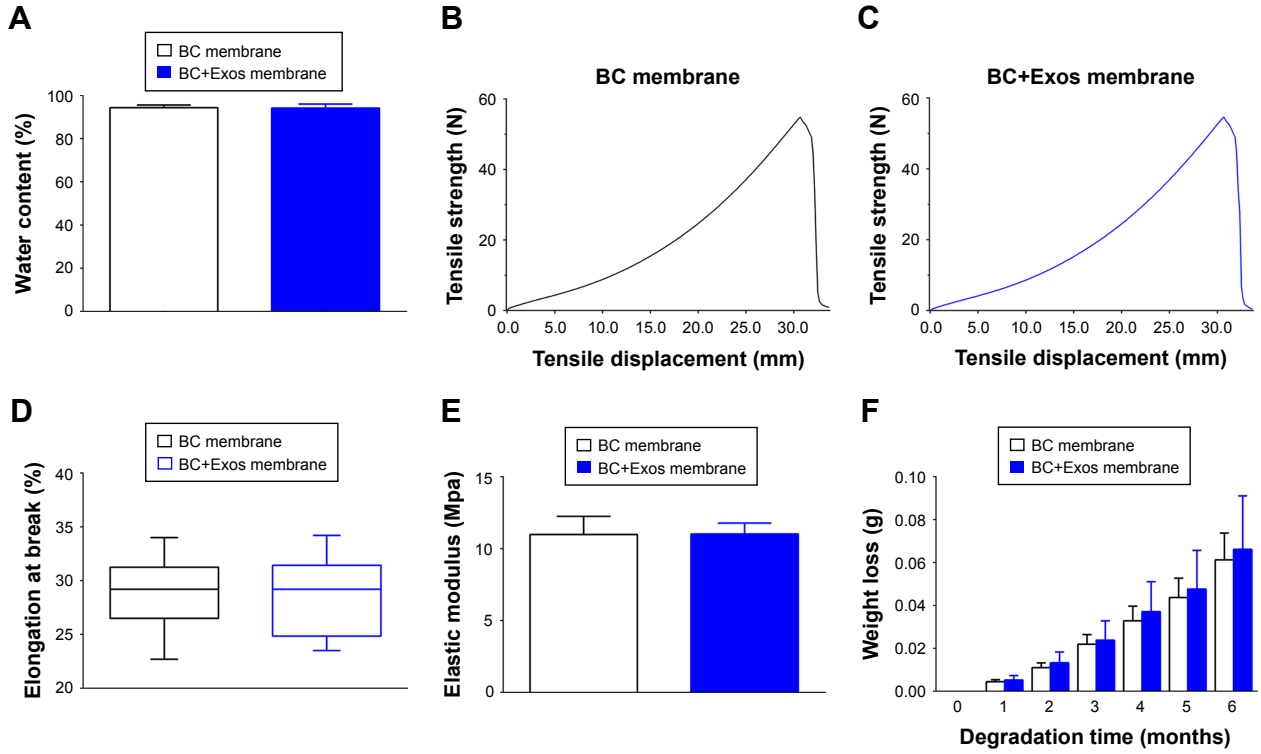

Figure 3 The properties of the BC membrane and the BC+Exos membrane.
Notes: (**A**) Water content. (**B** and **C**) Tensile strength of the BC membrane and the BC+Exos membrane, respectively. (**D**) Elongation at break. (**E**) Elastic modulus. (**F**) Degradation during 6 months.
Abbreviations: BC, bacterial cellulose; BC+Exos, bacterial cellulose combined with exosomes.

and 6 months in the BC membrane group, respectively. For the same period of degradation time, the weight loss in the BC membrane group and BC+Exos membrane group showed no significant difference (Figure 3F). All the results showed that both the BC and the BC+Exos membranes had almost no degradation in vitro during the test, and the BC+Exos membrane had stable properties and was capable of being applied in in vivo applications.

Biocompatibility in vitro and in vivo

The cytotoxicity evaluation of the BC and BC+Exos membranes in vitro was conducted by the observation of the live–dead cell staining. At 1, 3, and 5 days after the L929 cell was seeded on the membrane, the cells in all groups were attached well, and the cell density was gradually increased during the cultivation time (Figure 4A–J). Next, the cell proliferation rate was evaluated by the CCK-8 analysis. Figure 4K showed

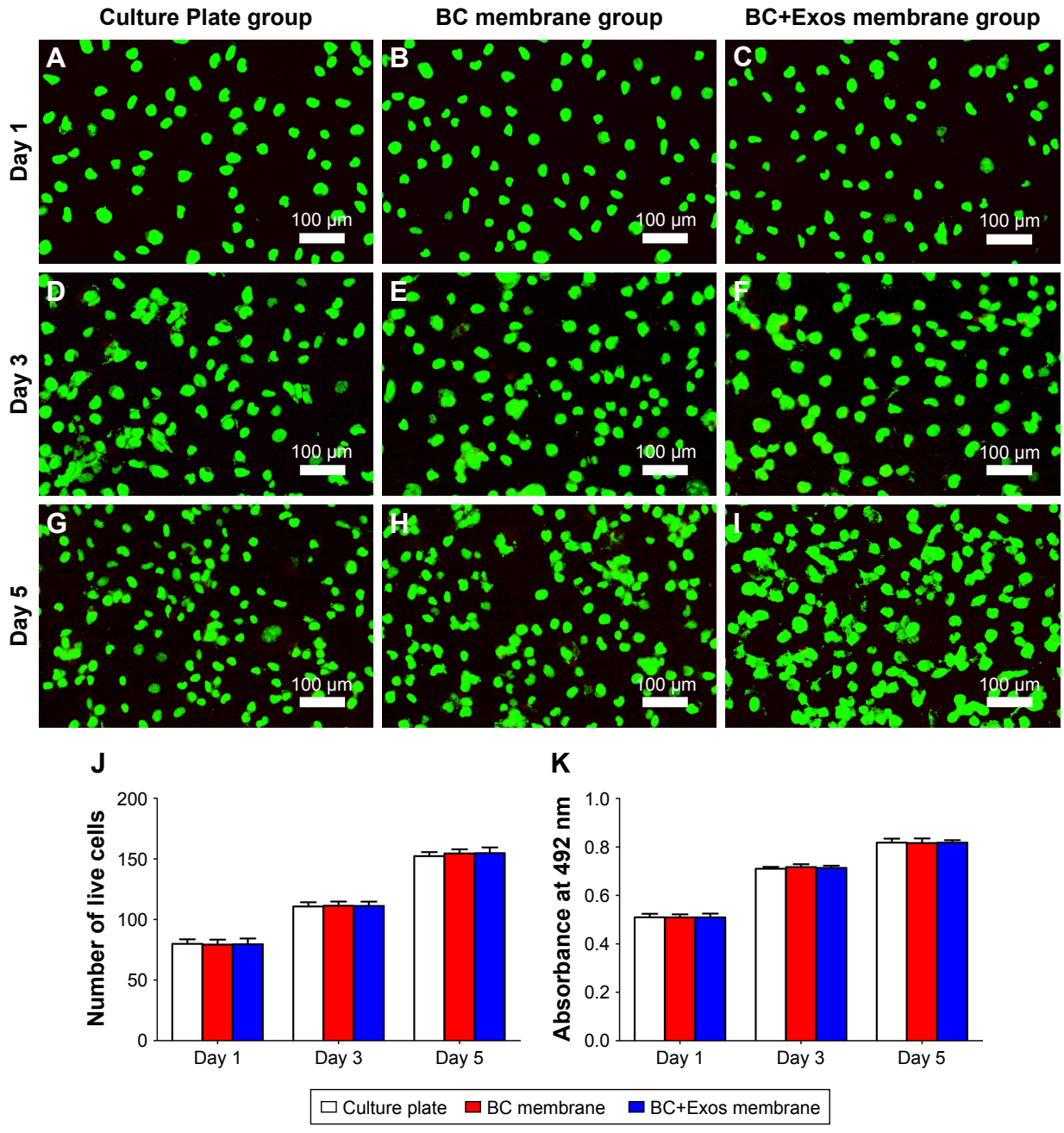

Figure 4 Biocompatibility of the BC+Exos membrane in vitro.
Notes: Representative images of live/dead cell staining at Day 1 (**A**–**C**), Day 3 (**D**–**F**), and Day 5 (**G**–**I**) in the culture plate, BC membrane group, and BC+Exos membrane group. The percentage of living cells (**J**) and CCK-8 values (**K**) in each group. All data were expressed as means ± standard error of mean.
Abbreviations: BC, bacterial cellulose; BC+Exos, bacterial cellulose combined with exosomes.

that the OD value in each group was increased gradually over time, and the OD value in each group was not statistically different at the same time. In addition, the biocompatibility of the BC+Exos membrane in vivo was detected at 7 days after operation. Figure 5A–D showed that there were no inflammatory cells, including monocytes, lymphocytes, and plasmacytes, observed at 7 days post operation in the muscle and subcutaneous tissues, suggesting that there was no acute inflammation and fibrous capsule formation in the early postoperative stage. Moreover, blood tests were conducted at days 1, 3, 7, 30, and 90 to assess the blood biocompatible effect of the BC+Exos membrane in rabbits. The values of ALT and AST are comparable well as markers of liver cell injury and are usually applied as indicators of liver function. In detail, the level of ALT in liver cells is sensitive to acute liver injury which is caused by alcohol or drugs, and the level of AST in liver cells is elevated in chronic hepatitis and cirrhosis.[33] The significant increase in BUN is probably attributable to impaired kidney function.[34] In addition, Scr has been introduced as the most frequently employed indicator to assess the glomerular filtration rate.[35]

In our study, the average ALT value in the control group and the BC membrane group at days 1 and 3 after surgery was higher than that at the preoperative time point; however, the average ALT was in a similar range at 7, 30, and 90 days postoperatively, as compared to that at the preoperative time point (Figure 5E). The average AST value in the control and BC+Exos membrane groups at 1 day after surgery was higher than that at the preoperative time point; however, the average AST was in a similar range at other time points postoperatively compared to that at the preoperative time point (Figure 5F). Moreover, the average BUN and Scr levels in the control and the BC+Exos membrane groups were in a similar range at any time point, compared to those at the preoperative time point (Figure 5G and H). In order to determine the long-term effect of the BC+Exos membrane on rabbits, the histology of heart, liver, and kidney of the rabbits was observed at 1 year post operation. The HE staining images showed that the heart, liver, and kidney had no tissue necrosis and displayed normal morphology (Figure 5I–K). All of the above findings suggested that the BC+Exos membrane was biocompatible both in vitro and in vivo.

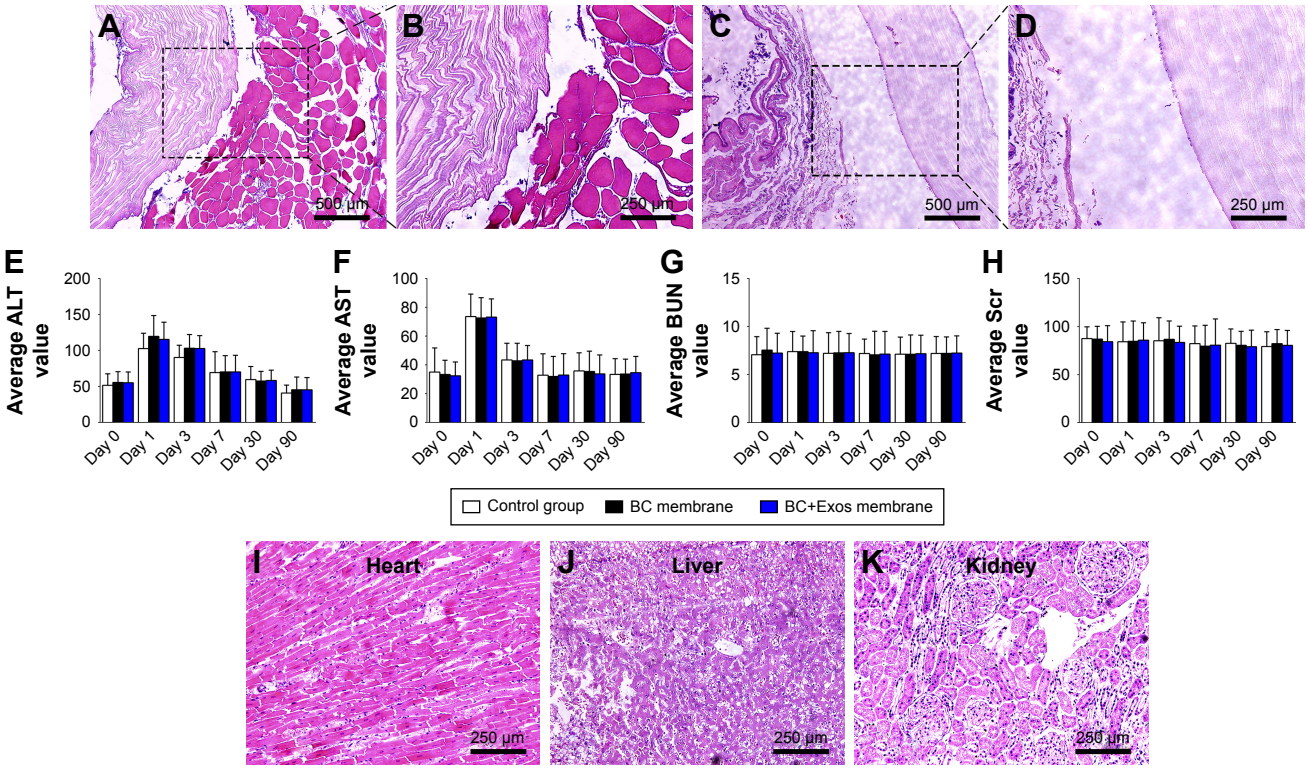

Figure 5 Biocompatibility of the BC+Exos membrane in vivo.

Notes: (**A** and **B**) Representative images of the area surrounding both the BC+Exos membrane and muscle at 1 week postoperatively. (**C** and **D**) Representative images of the area surrounding both the BC+Exos membrane and subcutaneous tissue at 1 week postoperatively. Blood tests of ALT (**E**), AST (**F**), BUN (**G**), and Scr (**H**) were conducted at days 1, 3, 7, 30, and 90 after surgery, respectively. Representative images of the long-term effect of the BC+Exos membrane on the heart (**I**), liver (**J**), and kidney (**K**).

Abbreviations: ALT, alanine aminotransferase; AST, aspartate aminotransferase; BC, bacterial cellulose; BC+Exos, bacterial cellulose combined with exosomes; BUN, blood urea nitrogen; Scr, serum creatinine.

The general view of the epidural fibrosis and adhesions

The degree of scar formation and dural adhesion in the surgical area was analyzed by a previously described method.[27] Figure 6A showed that the intensive scar formation was aggressively existent between the muscle and spinal cord, and the adherence was serious in the control group. Moreover, a slight membrane adherence was observed between the spinal membrane and the spinal cord in the ePTFE group (Figure 6B) and the BC membrane group (Figure 6D). In the PU membrane group (Figure 6C), some scars were dispersed under the membrane. However, there was almost no scar formation observed in the BC+Exos membrane group (Figure 6E); moreover, the area between the muscle and spinal cord was clear, indicating that the BC+Exos membrane was capable of preventing epidural fibrosis after surgery. Table 2 shows the number of rabbits in the different adhesion grades according to the adhesions grading scale in Table 4. The results suggested that compared with BC membrane group, the BC+Exos membrane group was found to significantly reduce the epidural fibrosis and adhesion postoperatively (P=0.009). The adhesion grades in the BC membrane group had no significant differences as compared with that in the ePTFE and PU groups. Moreover, the control group was found to have significantly massive fibrosis and severe adhesion. These results indicated that the BC+Exos

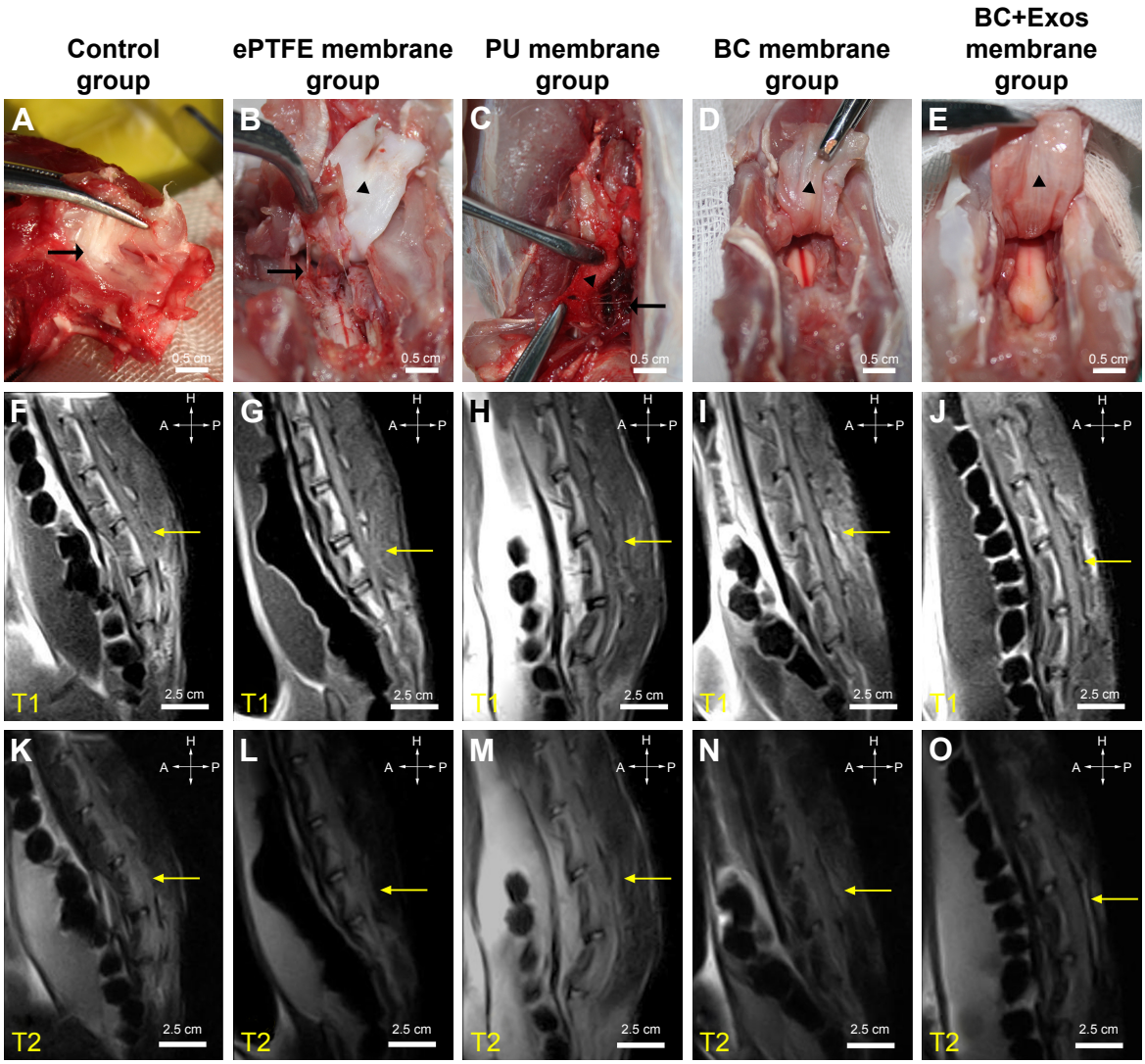

Figure 6 General view and MRI examination.

Notes: (**A**–**E**) At 1 year postoperatively, the general observation of the control, ePTFE membrane, PU membrane, BC membrane, and BC+Exos membrane groups, respectively. (**F**–**J**) At 1 year postoperatively, the T1-weighted MRI images of the control, ePTFE membrane, PU membrane, BC membrane, and BC+Exos membrane groups, respectively. (**K**–**O**) At 1 year postoperatively, the T2-weighted MRI images of the control, ePTFE membrane, PU membrane, BC membrane, and BC+Exos membrane groups, respectively.

Abbreviations: BC, bacterial cellulose; BC+Exos, bacterial cellulose combined with exosomes; ePTFE, expanded polytetrafluoroethylene; MRI, magnetic resonance image; PU, polyurethane.

Table 4 Postoperative adhesions grading scale

0	No adhesions
1	Firm fibrin adhesions, easily removed by blunt dissection (mild)
2	Fibrous adhesions, easily dissected (moderate)
3	Thick fibrous adhesions, dissectable (severe)
4	Thick fibrous adhesions, not dissectable without damage to the adherent tissue (very severe)

membrane could prevent epidural fibrosis and adhesion postoperatively.

The MRI scan

The sagittal examination of the spine was undertaken by MRI to evaluate the scar formation in the surgical area at 3 months after surgery. Figure 6F and K showed that the posterior epidural space disappeared and the scar was closely aligned with the spinal cord in the control group. The posterior epidural space was extant in the BC+Exos membrane group (Figure 6J), and the T2-weighted image showed a long strip T2 signal (Figure 6O); therefore, it may be that the BC+Exos film could separate the posterior epidural tissue from the spinal cord. The ePTFE and BC membrane groups showed that the posterior epidural space was extant (Figure 6G, I, L, and N); however, it was smaller than that in the BC+Exos membrane group, which suggested that the material could separate the posterior epidural tissue from the spinal cord. In addition, scar formation was observed in the PU membrane group (Figure 6H and M); however, it was not adherent to the spinal dura mater, and there was some postspinal dural space.

Histological examination

In order to assess the degree of epidural fibrosis and the inflammatory effect around the membrane, histology of the membrane and surrounding tissue was further conducted at 1 year after surgery. HE staining in Figure 7E and e showed that the space between the spinal dura mater and BC+Exos membrane was clear, without a visible scar, and there were no inflammatory cells infiltrated into the BC+Exos film surface. The collagen fiber was almost invisible on the Masson's trichrome stain (Figure 7J and j), and there were few type I collagen fibers observed on Sirius red staining (Figure 7O). In the PU membrane group, the fibroblasts had agminated between the spinal dura mater and PU membrane (Figure 7C and c), and some amount of collagen fibers were formed; moreover, these collagen fibers were observed by Masson's staining (Figure 7H and h) and Sirius red staining (Figure 7M). In addition, HE staining in the ePTFE membrane group displayed that fibroblasts were present in the area between the spinal dura mater and ePTFE membrane, and some collagen fibers were detected (Figure 7B and b); the Masson's trichrome staining (Figure 7G and g) and Sirius red staining (Figure 7L) revealed that collagen fibers were present between the spinal dura mater and the membrane. The BC membrane (Figure 7D, d, I, i, and N) showed a similar observational image compared to the ePTFE group. However, Figure 7A and a showed that fibroblasts were densely packed between the spinal cord and muscle, the collagen fiber was severely hyperplastic, which was closely adherent to the spinal dura mater, and the spinal cord was somewhat compressed in the control group. Moreover, Masson's trichrome and Sirius red staining showed that a large amount of type I collagen fibers was formed around the spinal cord (Figure 7F, f and K).

Expression of fibrosis-related genes

For further evaluation of the effects of the BC+Exos membrane on the characteristics of fibrosis-related gene expression in the surgical area, mRNA levels of *COL I*, *COL III*, and *α-SMA* were assessed by qRT-PCR at 4, 8, and 12 months after surgery. The mRNA levels of *COL I*, *COL III*, and *α-SMA* were in a similar range for the ePTFE membrane and PU membrane groups at 4, 8, and 12 months, respectively. As shown in Figure 8A, the *COL I* mRNA level in the BC+Exos membrane group at 4 months after surgery was 0.89- and 0.67-fold lower than that in the BC membrane and control group, respectively, at 8 months after surgery was 0.89- and 0.62-fold lower than that in the BC membrane and control groups, respectively, and at 12 months after surgery was 0.89- and 0.55-fold lower than that in the BC membrane and control groups, respectively. The *COL III* mRNA level in the BC+Exos membrane group at 4 months after surgery was 0.89- and 0.66-fold lower than that in the BC membrane and control groups, respectively, at 8 months after surgery was 0.87- and 0.59-fold lower than that in the BC membrane and control groups, respectively, and, at 12 months after surgery, it was 0.84- and 0.53-fold lower than that in the BC membrane and control groups, respectively (Figure 8B). The *α-SMA* mRNA level in the BC+Exos membrane group at 4 months after surgery was 0.92- and 0.77-fold lower than that in the BC membrane and control groups, respectively; at 8 months after surgery, it was 0.91- and 0.71-fold lower than that in the BC membrane and control groups, respectively; and, at 12 months after surgery, it was 0.93- and 0.67-fold lower than that in the BC membrane and control groups, respectively (Figure 8C). Moreover, the mRNA levels of *COL I*, *COL III*, and *α-SMA* in the BC membrane group

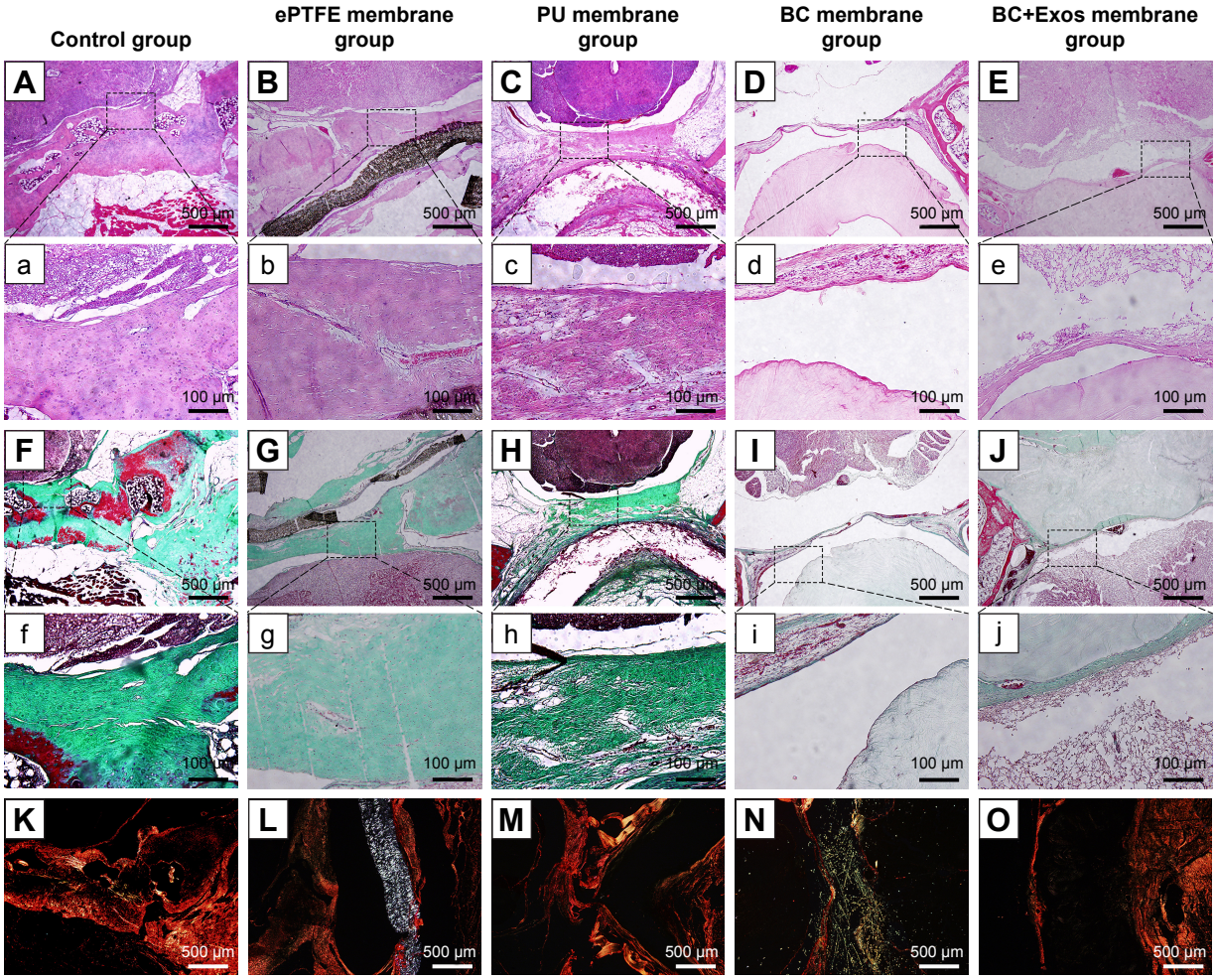

Figure 7 Histological examination.
Notes: (**A**, a, **B**, b, **C**, c, **D**, d, **E**, and e) The HE staining images of the control, ePTFE membrane, PU membrane, BC membrane, and BC+Exos membrane groups at 1 year post operation, respectively. (**F**, f, **G**, g, **H**, h, **I**, i, **J**, and j) The Masson trichrome images of the control, ePTFE membrane, PU membrane, BC membrane, and BC+Exos membrane groups at 1 year post operation, respectively. (**K**–**O**) The Sirius red staining of the control, ePTFE membrane, PU membrane, BC membrane, and BC+Exos membrane groups at 1 year post operation, respectively.
Abbreviations: BC, bacterial cellulose; BC+Exos, bacterial cellulose combined with exosomes; ePTFE, expanded polytetrafluoroethylene; MRI, magnetic resonance image; PU, polyurethane.

were significantly lower than that in the ePTFE membrane and PU membrane groups, respectively.

Discussion

In the present study, we first developed a novel BC+Exos membrane which was composed of BC membrane and HUCMSCs-exosomes, and then detected the characterization and biocompatibility of the membrane both in vitro and in vivo; finally, the BC+Exos membrane was sutured after laminectomy in rabbits to prevent epidural scar formation. To our knowledge, this is the first study on the prevention of epidural fibrosis after laminectomy by using a HUCMSCs-Exos-based BC membrane. These findings open up a new strategy for preventing epidural fibrosis after laminectomy with this BC+Exos membrane through reduced fibroblast infiltration and collagen fiber formation.

Epidural scar formation is an inevitable process after laminectomy, and excessive epidural fibrosis can lead to FBSS, which can further induce recurrent pain or neurological dysfunction.[36] The possible mechanism of the epidural scar formation is that the fibroblasts around the surgical environment are transported into the operative area by blood, causing epidural fibrosis.[37] Therefore, the main strategy for preventing epidural fibrosis is to restrict the migration of fibroblasts, ensure thorough hemostasis in the surgical area, and isolate the contact of the spinal dura mater and fibrous tissue. Recently, it has been widely believed that establishing a physical barrier between the spinal dura mater and posterior tissue by biomaterials is an effective approach to

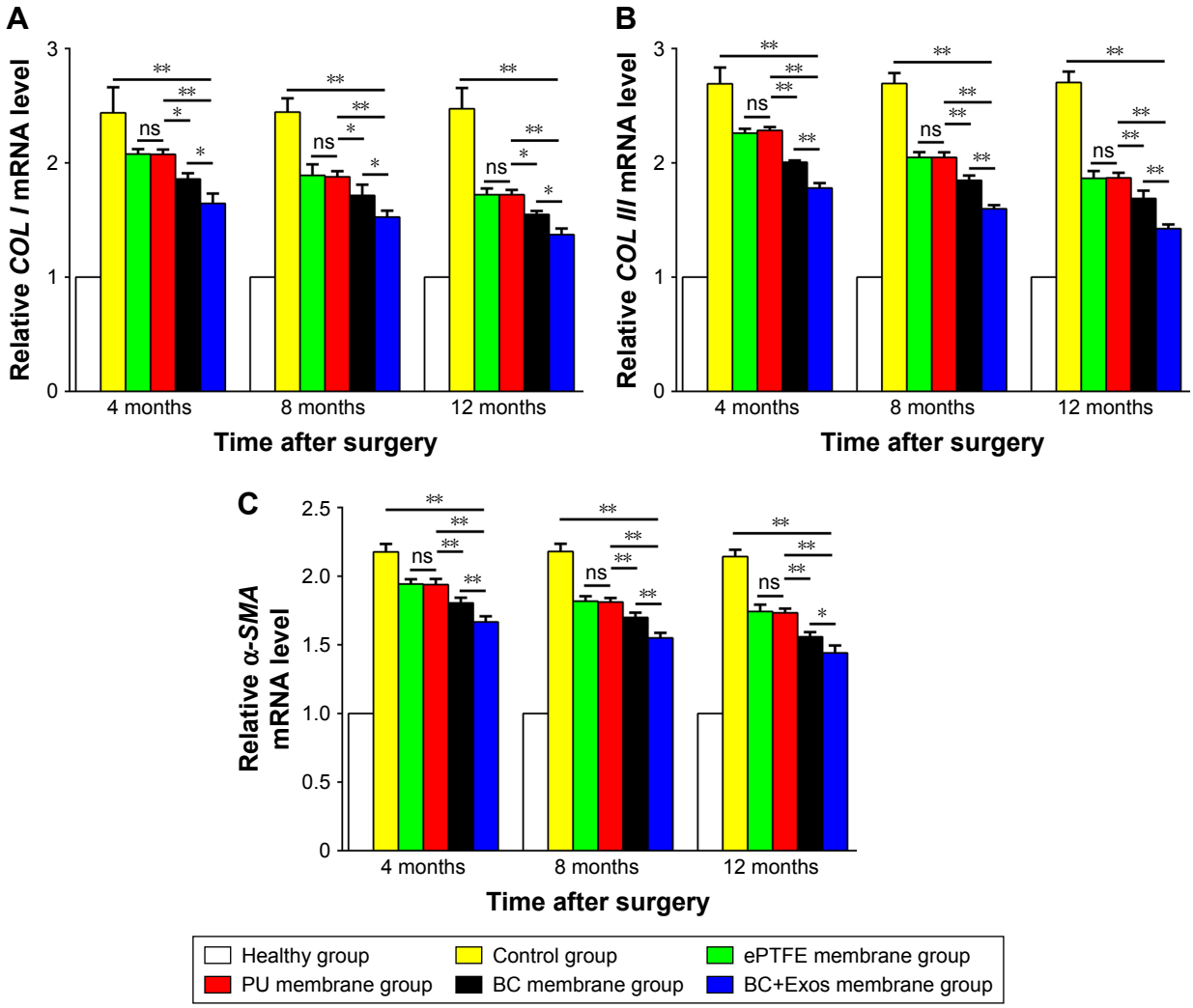

Figure 8 The mRNA levels of fibrosis-related genes.

Notes: The mRNA levels of (**A**) *COL I*, (**B**) *COL III*, and (**C**) α-*SMA* were determined for the healthy, control, ePTFE membrane, PU membrane, BC membrane, and BC+Exos membrane groups at 4, 8, and 12 months post operation. Each assay was repeated three times. All data are expressed as means ± standard error of mean. $^{*}P<0.05$, $^{**}P<0.01$.

Abbreviations: α-SMA, alpha smooth muscle actin; BC, bacterial cellulose; BC+Exos, bacterial cellulose combined with exosomes; COL I, collagen type I; COL III, collagen type III; ePTFE, expanded polytetrafluoroethylene; mRNA, messenger ribonucleic acid; ns, not significant; PU, polyurethane.

reduce fibroblast infiltration and scar tissue formation, and, finally, to prevent epidural fibrosis formation.[38] In the present study, we fabricated a BC+Exos membrane by using the following procedure. The BC membrane was first cultivated from acetobacterxylinum – a gram-negative bacterium that possesses the ability to synthesize large amounts of high-quality cellulose.[39] The bacteria are capable of absorbing sugar from the culture medium and developing linear β–1,4-glucose chains which are secreted into the surface of bacteria through the mycoderm pores; then, the glucose chains on the bacteria surface are aggregated into the subfibrils and microfibers, and the HUCMSCs-exosomes were introduced into the process, which finally form a membranous structure in a static environment.[29,40]

The BC+Exos membranes we fabricated in the present study were arrayed into 3D structure as seen under SEM and aligned with strong tensile strength and elongation of breaks, thereby conferring high cellulose crystallinity and proper mechanical strength to the BC membrane. The elastic modulus of the BC+Exos membrane could reach 11 MPa, which was approximate to the elastic modulus of articular cartilage. In addition, the even fiber diameter and high water content of the BC+Exos membrane ensured it possessed a bigger inner space and favorable elasticity and adhesiveness and, therefore, was capable of adhering to an anomalous surface. Moreover, the moderate porosity of the BC+Exos membrane facilitated the substance exchange in the wound environment. All these findings indicate that the BC+Exos

membrane is capable of being a promising substance in preventing epidural fibrosis with its moderate mechanical performance and physicochemical properties.

Biodegradation and biocompatibility of the membrane are two critical parameters for their application in preventing epidural fibrosis. Therefore, the authors examined in vitro degradation and cytotoxity in experiments, as well as the in vivo tissue response and blood effect of the ambient tissues and viscera to the membrane. The degradation experiment of the BC+Exos membrane in the simulated body fluids showed that the BC+Exos film was not degradable in vitro, and the membrane possessed stable characteristics and was capable of being introduced into in vivo application. Next, the biocompatibility of the BC+Exos membrane in vitro was detected by L929 cells, which are one of the standard cells in cytotoxicity tests.[41,42] The light microscopy photographs of L929 cells co-cultivated with different concentrations of the extraction from the BC membrane at 1, 3, and 5 days showed that cells in all groups were attached well and appeared triangular or spindle-shaped, the cell morphology rating in each concentration of the extraction being nontoxic. Moreover, the CCK-8 experiment expressed the phenomenon that the OD value had no significant differences between each group at the same time point. All of these findings implied that the BC+Exos membrane had no cytotoxicity in vitro and could be introduced into in vivo application. In addition, the biocompatibility of the BC+Exos membrane in vivo was investigated by histological examination and blood test. The HE staining images in the early postoperative period showed that there was no acute inflammation in the BC+Exos membrane group. The levels of ALT and AST were higher in the first or 3 days after surgery, and returned to normal level at 7 days postoperatively; this might be attributable to the introduction of anesthetics and antibiotics. Moreover, the levels of the blood tests at other time points had no significant difference between the BC+Exos membrane group and other groups ($P>0.05$). For long-term biocompatibility, we conducted histological examination of the heart, liver, and kidney. The HE images showed that these organs had no visible necrosis and inflammation in the BC+Exos membrane. In addition, the inflammatory cells were not infiltrated into the BC+Exos membrane and its surrounding tissues. All these findings suggested that the BC+Exos membrane possessed stable biocompatibility in both short-term and long-term periods; however, further studies are needed to evaluate the genetic toxicity and blood compatibility tests, in order to confirm the biosafety of the membrane in all aspects.

Next, we tested the effects of the BC+Exos membrane in preventing epidural fibrosis. The ePTFE (Core Technologies, USA) spinal membrane and PU (B. Braun Medical Inc., USA) nerve patch were introduced into the experiment as positive controls. The ePTFE membrane has proper stability, wear resistance, and excellent biocompatibility.[43] It has been used as a substitute material in clinical application in artificial blood vessels.[44] Moreover, the ePTFE spinal membrane which was developed by Core Technologies has been proven to be an effective physical barrier in preventing scar formation as well as adhesion and compression on the spinal dura mater after spinal surgery. Moreover, the PU nerve patch has appropriate physicochemical properties and bio-stability and is capable of preventing epidural adhesion as a permanent substitute. MRI examination is an effective and noninvasive approach to observe the degree of epidural fibrosis. In the present study, the T2-weighted sagittal images were more appropriately used to evaluate the scar tissue.[45] The images showed that the scar formation was significantly obvious in the control group compared to the other groups, the epidural adhesion was tight, and the spinal cord was compressed to varying degrees. However, the T2-weighted images showed that the posterior epidural space was similar in the ePTFE and BC membrane groups, which was smaller than in the BC+Exos membrane group but larger than in the PU group. In addition, the adhesion grading scale suggested that the BC+Exos membrane group had significant differences as compared to the other four groups. In order to assess the collagen fibers, Masson's trichrome and Sirius red stains were applied in the histological analysis. In the control group, the green and blue collagen fibers were intensive and were tightly closed between the epidural mater and muscle, and a large number of red and yellow type I collagen fibers were observed under polarized light, and the histopathological degree was grade 3, which was the most severe characterization of epidural fibrosis according to the previous studies.[46,47] In other groups, the dural mater was isolated from the rear tissue by the membrane, and there were a small amount of collagenous fibers between the dural mater and the material; most importantly, the BC+Exos membrane group possessed a minimal quantity of collagen fibers, which might be attributed to the fact that the stickiness of the BC+Exos membrane was better than that of the other membranes, which was close to the lamina and surrounding tissues, and its physical isolation was the best.

During the formation of epidural fibrosis, several complicated pathophysiologic changes, such as enhanced expression of inflammatory cytokines, increased proliferation of fibroblasts, and hypernomic production of collagens

(eg, *COL I* and *COL III*) and *α-SMA*, were introduced into the process.[48–51] In this study, the expression of *COL I*, *COL III*, and *α-SMA* was detected. The results showed that the expression of fibrosis-related genes of the BC membrane was significantly lower than that in other groups, excluding the BC+Exos membrane group, at 4, 8, and 12 months after laminectomy; moreover, when the HUCMSC-Exos were added into the BC membrane to fabricate the BC+Exos membrane, the mRNA levels of *COL I*, *COL III*, and *α-SMA* were significantly lower than that in the BC membrane group, indicating that the HUCMSC-Exos and BC membrane worked synergistically to prevent the epidural fibrosis.

Although the mechanism by which the BC+Exos membranes prevent the epidural fibrosis and adhesion is unknown, a few feasible explanation can be discussed. Previous studies have suggested that HUCMSC-Exos undertake functions by miRNAs in various biological and pathological processes.[52–54] miRNAs are a type of small non-coding RNAs which can bind to mRNAs and act as regulators of mRNA expression and translational efficiency.[55] Moreover, miRNAs–mRNAs can give rise to the recruitment of the targeted mRNAs to the RNA-induced silencing complex, thereby introducing translational arrest and mRNA degradation, and finally decrease protein expression of target mRNAs.[56,57] Therefore, this led us to hypothesize that HUCMSCs secrete exosomal miRNAs, which serve as a compositional substance of membrane materials that can regulate the fibroblast infiltration and the scar tissue, and finally prevent epidural fibrosis formation. Further studies are needed to investigate the exact mechanism underlying the positive prevention effect of the BC+Exos membrane on epidural fibrosis after laminectomy.

Conclusion

The present study illustrates a novel membrane, which was composed of exosomes and BC, in positively preventing epidural fibrosis. The BC+Exos membrane holds 3D network structures, has modest physiochemical properties, and possesses a tunable biocompatibility both in vitro and in vivo, thus making it appropriate for supporting the space between the dural mater and surrounding tissues. The HUCMSCs-exosomes which were mixed into the BC membrane work synergistically to reduce fibrosis after laminectomy. These findings highlight the possibilities of the prevention of epidural fibrosis after lumbar surgery.

Acknowledgments

This work was supported by grants from the National Natural Science Foundation of China (51772328) and the Science and Technology Plan of Beijing City (Z161100001516013). Bo Wang is now affiliated with the Department of Trauma and Orthopedics, Peking University People's Hospital, Beijing, 100044, China.

Disclosure

The authors report no conflicts of interest in this work.

References

1. Thomson S. Failed back surgery syndrome – definition, epidemiology and demographics. *Br J Pain*. 2013;7(1):56–59.
2. Skaf G, Bouclaous C, Alaraj A, Chamoun R. Clinical outcome of surgical treatment of failed back surgery syndrome. *Surg Neurol*. 2005;64(6):483–488.
3. Ido K, Urushidani H. Fibrous adhesive entrapment of lumbosacral nerve roots as a cause of sciatica. *Spinal Cord*. 2001;39(5):269–273.
4. Richter HP, Kast E, Tomczak R, Besenfelder W, Gaus W. Results of applying ADCON-L gel after lumbar discectomy: the German ADCON-L study. *J Neurosurg*. 2001;95(2 Suppl):179–189.
5. Liu LS, Berg RA. Adhesion barriers of carboxymethylcellulose and polyethylene oxide composite gels. *J Biomed Mater Res*. 2002;63(3):326–332.
6. Preul MC, Campbell PK, Garlick DS, Spetzler RF. Application of a new hydrogel dural sealant that reduces epidural adhesion formation: evaluation in a large animal laminectomy model. *J Neurosurg Spine*. 2010;12(4):381–390.
7. Isık S, Taşkapılıoğlu MÖ, Atalay FO, Dogan S. Effects of cross-linked high-molecular-weight hyaluronic acid on epidural fibrosis: experimental study. *J Neurosurg Spine*. 2015;22(1):94–100.
8. Li C, Wang H, Liu H, et al. The prevention effect of poly (L-glutamic acid)/chitosan on spinal epidural fibrosis and peridural adhesion in the post-laminectomy rabbit model. *Eur Spine J*. 2014;23(11):2423–2431.
9. Le AX, Rogers DE, Dawson EG, et al. Unrecognized durotomy after lumbar discectomy: a report of four cases associated with the use of ADCON-L. *Spine (Phila Pa 1976)*. 2001;26(1):115–117.
10. Xu J, Chen Y, Yue Y, Sun J, Cui L. Reconstruction of epidural fat with engineered adipose tissue from adipose derived stem cells and PLGA in the rabbit dorsal laminectomy model. *Biomaterials*. 2012;33(29):6965–6973.
11. Zhang C, Yin X, Zhang J, et al. Clinical observation of umbilical cord mesenchymal stem cell treatment of severe idiopathic pulmonary fibrosis: A case report. *Exp Ther Med*. 2017;13(5):1922–1926.
12. Kim A, Yu HY, Heo J, et al. Mesenchymal stem cells protect against the tissue fibrosis of ketamine-induced cystitis in rat bladder. *Sci Rep*. 2016;6:30881.
13. Oh W, Kim DS, Yang YS, Lee JK. Immunological properties of umbilical cord blood-derived mesenchymal stromal cells. *Cell Immunol*. 2008;251(2):116–123.
14. Reinisch A, Bartmann C, Rohde E, et al. Humanized system to propagate cord blood-derived multipotent mesenchymal stromal cells for clinical application. *Regen Med*. 2007;2(4):371–382.
15. Eggenhofer E, Luk F, Dahlke MH, Hoogduijn MJ. The life and fate of mesenchymal stem cells. *Front Immunol*. 2014;5:148.
16. Zou X, Gu D, Xing X, et al. Human mesenchymal stromal cell-derived extracellular vesicles alleviate renal ischemic reperfusion injury and enhance angiogenesis in rats. *Am J Transl Res*. 2016;8(10):4289–4299.
17. Liu B, Ding F, Hu D, et al. Human umbilical cord mesenchymal stem cell conditioned medium attenuates renal fibrosis by reducing inflammation and epithelial-to-mesenchymal transition via the TLR4/NF-κB signaling pathway in vivo and in vitro. *Stem Cell Res Ther*. 2018;9(1):7.
18. Costa-Silva B, Aiello NM, Ocean AJ, et al. Pancreatic cancer exosomes initiate pre-metastatic niche formation in the liver. *Nat Cell Biol*. 2015;17(6):816–826.
19. Zhang L, Zhang S, Yao J, et al. Microenvironment-induced PTEN loss by exosomal microRNA primes brain metastasis outgrowth. *Nature*. 2015;527(7576):100–104.

20. Ying W, Riopel M, Bandyopadhyay G, et al. Adipose Tissue Macrophage-Derived Exosomal miRNAs Can Modulate In Vivo and In Vitro Insulin Sensitivity. *Cell*. 2017;171(2):372–384.
21. Borges FT, Melo SA, Özdemir BC, et al. TGF-β1-containing exosomes from injured epithelial cells activate fibroblasts to initiate tissue regenerative responses and fibrosis. *J Am Soc Nephrol*. 2013;24(3):385–392.
22. Solé C, Cortés-Hernández J, Felip ML, Vidal M, Ordi-Ros J. miR-29c in urinary exosomes as predictor of early renal fibrosis in lupus nephritis. *Nephrol Dial Transplant*. 2015;30(9):1488–1496.
23. Li T, Yan Y, Wang B, et al. Exosomes derived from human umbilical cord mesenchymal stem cells alleviate liver fibrosis. *Stem Cells Dev*. 2013;22(6):845–854.
24. Fiore EJ, Mazzolini G, Aquino JB. Mesenchymal Stem/Stromal Cells in Liver Fibrosis: Recent Findings, Old/New Caveats and Future Perspectives. *Stem Cell Rev*. 2015;11(4):586–597.
25. Cervio E, Barile L, Moccetti T, Vassalli G. Exosomes for Intramyocardial Intercellular Communication. *Stem Cells Int*. 2015;2015:482171.
26. Liu Z, Zhu S, Liu L, et al. A magnetically responsive nanocomposite scaffold combined with Schwann cells promotes sciatic nerve regeneration upon exposure to magnetic field. *Int J Nanomedicine*. 2017;12:7815–7832.
27. Einhaus SL, Robertson JT, Dohan FC, Wujek JR, Ahmad S, Dohan CF Jr. Reduction of peridural fibrosis after lumbar laminotomy and discectomy in dogs by a resorbable gel (ADCON-L). *Spine (Phila Pa 1976)*. 1997;22(13):1440–1446.
28. Lo HY, Kuo HT, Huang YY. Application of polycaprolactone as an anti-adhesion biomaterial film. *Artif Organs*. 2010;34(8):648–653.
29. Czaja W, Romanovicz D, Brown R. Structural investigations of microbial cellulose produced in stationary and agitated culture. *Cellulose*. 2004;11(3/4):403–411.
30. Shinkawa T, Tang X, Gossett JM, et al. Valved Polytetrafluoroethylene Conduits for Right Ventricular Outflow Tract Reconstruction. *Ann Thorac Surg*. 2015;100(1):129–137.
31. Caimmi PP, Sabbatini M, Fusaro L, Borrone A, Cannas M. A study of the mechanical properties of ePTFE suture used as artificial mitral chordae. *J Card Surg*. 2016;31(8):498–502.
32. Svensson A, Nicklasson E, Harrah T, et al. Bacterial cellulose as a potential scaffold for tissue engineering of cartilage. *Biomaterials*. 2005;26(4):419–431.
33. Zhang XD, Wu D, Shen X, et al. In vivo renal clearance, biodistribution, toxicity of gold nanoclusters. *Biomaterials*. 2012;33(18):4628–4638.
34. Shavit L, Lifschitz M, Galperin I. Influence of enteric nutrition on blood urea nitrogen (BUN) in very old patients with chronic kidney disease (CKD). *Arch Gerontol Geriatr*. 2012;54(1):228–231.
35. Qu N, Lee RJ, Sun Y, et al. Cabazitaxel-loaded human serum albumin nanoparticles as a therapeutic agent against prostate cancer. *Int J Nanomedicine*. 2016;11:3451–3459.
36. Ross JS, Robertson JT, Frederickson RC, et al. Association between peridural scar and recurrent radicular pain after lumbar discectomy: magnetic resonance evaluation. ADCON-L European Study Group. *Neurosurgery*. 1996;38(4):855–863.
37. Slipman CW, Shin CH, Patel RK, et al. Etiologies of failed back surgery syndrome. *Pain Med*. 2002;3(3):200–214.
38. Alkalay RN, Kim DH, Urry DW, et al. Prevention of postlaminectomy epidural fibrosis using bioelastic materials. *Spine (Phila Pa 1976)*. 2003;28(15):1659–1665.
39. Brown RM, Willison JH, Richardson CL. Cellulose biosynthesis in Acetobacter xylinum: visualization of the site of synthesis and direct measurement of the in vivo process. *Proc Natl Acad Sci U S A*. 1976;73(12):4565–4569.
40. Ross P, Mayer R, Benziman M. Cellulose biosynthesis and function in bacteria. *Microbiol Rev*. 1991;55(1):35–58.
41. International Organization for Standardization. *ISO-10993-5:2009(E) I, Biological Evaluation of Medical Devices – Part 5:Tests for in Vitro Cytotoxicity*. Geneva: International Organization for Standardization; 2009.
42. Richardson RR, Miller JA, Reichert WM. Polyimides as biomaterials: preliminary biocompatibility testing. *Biomaterials*. 1993;14(8):627–635.
43. Biswas SK, Vijayan K. Friction and wear of PTFE – a review. *Wear*. 1992;158(1–2):193–211.
44. Klinkert P, Post PN, Breslau PJ, van Bockel JH. Saphenous vein versus PTFE for above-knee femoropopliteal bypass. A review of the literature. *Eur J Vasc Endovasc Surg*. 2004;27(4):357–362.
45. Su C, Yao C, Lu S, et al. Study on the optimal concentration of topical mitomycin-C in preventing postlaminectomy epidural adhesion. *Eur J Pharmacol*. 2010;640(1–3):63–67.
46. He Y, Revel M, Loty B. A quantitative model of post-laminectomy scar formation. Effects of a nonsteroidal anti-inflammatory drug. *Spine (Phila Pa 1976)*. 1995;20(5):557–563.
47. Rydell N. Decreased granulation tissue reaction after installment of hyaluronic acid. *Acta Orthop Scand*. 1970;41(3):307–311.
48. Spiegelberg L, Swagemakers SM, van Ijcken WF, et al. Gene expression analysis reveals inhibition of radiation-induced TGFβ-signaling by hyperbaric oxygen therapy in mouse salivary glands. *Mol Med*. 2014;20:257–269.
49. Fan X, Chen J, Shi D, et al. The role and mechanisms of action of SIRT6 in the suppression of postoperative epidural scar formation. *Int J Mol Med*. 2016;37(5):1337–1344.
50. Jun JI, Lau LF. The matricellular protein CCN1 induces fibroblast senescence and restricts fibrosis in cutaneous wound healing. *Nat Cell Biol*. 2010;12(7):676–685.
51. Xu Q, Zhou W, Kong HY, et al. The effect of the Sanqi qisodium hyaluronate gel on the collagen of epidural scar after rabbits laminectomy. *Zhongguo Gu Shang*. 2010;23(4):278–281.
52. Li X, Liu L, Yang J, et al. Exosome Derived From Human Umbilical Cord Mesenchymal Stem Cell Mediates miR-181c Attenuating Burn-induced Excessive Inflammation. *EBioMedicine*. 2016;8:72–82.
53. Sun L, Li D, Song K, et al. Exosomes derived from human umbilical cord mesenchymal stem cells protect against cisplatin-induced ovarian granulosa cell stress and apoptosis in vitro. *Sci Rep*. 2017;7(1):2552.
54. Ti D, Hao H, Fu X, Han W. Mesenchymal stem cells-derived exosomal microRNAs contribute to wound inflammation. *Sci China Life Sci*. 2016;59(12):1305–1312.
55. Bartel DP. MicroRNAs: genomics, biogenesis, mechanism, and function. *Cell*. 2004;116(2):281–297.
56. Ameres SL, Martinez J, Schroeder R. Molecular basis for target RNA recognition and cleavage by human RISC. *Cell*. 2007;130(1):101–112.
57. Mallory AC, Reinhart BJ, Jones-Rhoades MW, et al. MicroRNA control of PHABULOSA in leaf development: importance of pairing to the microRNA 5′ region. *EMBO J*. 2004;23(16):3356–3364.